

Weak localization and weak anti-localization in topological insulators

Hai-Zhou Lu and Shun-Qing Shen

Department of Physics, The University of Hong Kong, Pokfulam Road, Hong Kong, China

ABSTRACT

Weak localization and weak anti-localization are quantum interference effects in quantum transport in a disordered electron system. Weak anti-localization enhances the conductivity and weak localization suppresses the conductivity with decreasing temperature at very low temperatures. A magnetic field can destroy the quantum interference effect, giving rise to a cusp-like positive and negative magnetoconductivity as the signatures of weak localization and weak anti-localization, respectively. These effects have been widely observed in topological insulators. In this article, we review recent progresses in both theory and experiment of weak (anti-)localization in topological insulators, where the quasiparticles are described as Dirac fermions. We predicted a crossover from weak anti-localization to weak localization if the massless Dirac fermions (such as the surface states of topological insulator) acquire a Dirac mass, which was confirmed experimentally. The bulk states in a topological insulator thin film can exhibit the weak localization effect, quite different from other system with strong spin-orbit interaction. We compare the localization behaviors of Dirac fermions with conventional electron systems in the presence of disorders of different symmetries. Finally, we show that both the interaction and quantum interference are required to account for the experimentally observed temperature and magnetic field dependence of the conductivity at low temperatures.

Keywords: Topological insulator, Weak localization, Weak anti-localization, Surface states

Contents

1	INTRODUCTION	2
2	WEAK LOCALIZATION AND ANTI-LOCALIZATION	2
2.1	Quantum diffusion	2
2.2	Signatures of weak (anti-)localization	3
2.3	Weak anti-localization in topological insulators	3
3	WEAK ANTI-LOCALIZATION AND LOCALIZATION CROSSOVER	4
3.1	Theoretical formalism	4
3.2	Experimental verification	5
4	WEAK LOCALIZATION OF BULK STATES	5
5	COMPARISON WITH CONVENTIONAL ELECTRONS	6
6	INTERACTION-INDUCED LOCALIZATION OF SURFACE ELECTRONS	7
6.1	Transport paradox in measurements	7
6.2	Theory of interaction effect	7
7	SUMMARY	9

1. INTRODUCTION

Topological insulators are gapped band insulators with topologically protected gapless modes surrounding their boundaries.^{1–4} The surface states of a three-dimensional topological insulator are composed of an odd number of two-dimensional gapless Dirac cones, which has a helical spin structure in momentum space,⁵ giving rise to a π Berry phase when an electron moves adiabatically around the Fermi surface. The π Berry phase can lead to the absence of backscattering,⁶ and further delocalization of the surface electrons.^{7,8} Because of these properties, the topological insulators are believed to have better performance in future electronic devices, thus have attracted much interest in studying their transport properties.^{9,10}

In experiments, the delocalization of electrons was believed to be verified by a phenomenon named the weak anti-localization.¹¹ The effect stems from the π Berry phase,¹² which induces a destructive quantum interference between time-reversed loops formed by scattering trajectories. The destructive interference can suppress backscattering of electrons, then the conductivity is enhanced with decreasing temperature because decoherence mechanisms are suppressed at low temperatures.^{13,14} A magnetic field can destroy the interference as well as the enhanced conductivity, so the signature of the weak anti-localization is a negative magnetoconductivity, which has been observed in a lot of topological insulator samples.^{15–21}

Having topologically protected surface states that cannot be localized is one of the alternative definitions of the topological insulators,^{1,2} and this is regarded as one of the merits of a topological insulator compared to ordinary metals. However, the metallic enhancement in conductivity expected to appear along with the negative magnetoconductivity is not observed at low temperatures. Instead, in most experiments, a logarithmic suppression of the conductivity with decreasing temperature is observed,^{22–27} indicating a behavior of the weak localization, which was supposed to occur in ordinary disordered metals as a precursor of the Anderson localization,^{28,29} which was known as a transport paradox in topological insulators.

Here we review our recent efforts^{30–33} on the theoretical understanding to the weak localization and weak anti-localization effects in the transport experiments in topological insulators. In Sec. 2, we give an introduction to the quantum diffusion regime, where the weak (anti-)localization happens. Then the experiments of weak anti-localization in topological insulators are reviewed. In Sec. 3, we discuss the crossover between weak anti-localization and weak localization and the Berry phase argument. In Sec. 4, we show why the bulk states in topological insulator can have weak localization. In Sec. 5, we compare the Dirac fermions with conventional electrons, on their localization behaviors in the presence of three kinds of disorder scattering. In Sec. 6, we will explain how the contradictory observations in the temperature and magnetic field dependence of the conductivity of topological insulators can be understood, by including both the quantum interference and electron-electron interactions for the disordered Dirac fermions.

2. WEAK LOCALIZATION AND ANTI-LOCALIZATION

2.1 Quantum diffusion

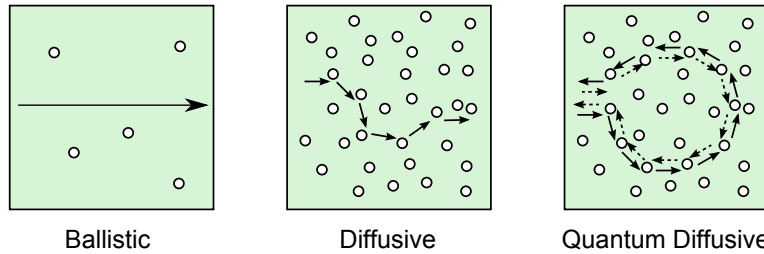


Figure 1. Schematic illustration of different electronic transport regimes in solids. The open circles represent impurities and arrows mark the trajectories that electron travelled.

The electronic transport in solids can be classified by several characteristic lengths: (i) The mean free path ℓ , which measures the average distance that an electron travels before its momentum is changed by elastic scattering from static scattering centers. (ii) The phase coherence length ℓ_ϕ , which measures the average distance an electron

can maintain its phase coherence. ℓ_ϕ is usually determined by inelastic scattering from electron-phonon coupling and interaction with other electrons. (iii) The sample size L .

If $\ell \gg L$, electrons can tunnel through the sample without being scattered. This is the ballistic transport regime. In the opposite limit $\ell \ll L$, electrons will suffer from scattering and diffuse through the sample, and this is the diffusive transport regime. In the diffusive regime, if $\ell_\phi \leq \ell$, we call it the semiclassical diffusion, and this part gives the Drude conductivity. If $\ell_\phi \gg \ell$, electrons will maintain their phase coherence even after being scattered for many times, referring to as the quantum diffusive regime. In this regime, the quantum interference between time-reversed scattering loops (see Fig. 1) will give rise to a correction to the conductivity. The weak localization or weak anti-localization is an effect due to this correction in the conductivity in the quantum diffusive regime.

2.2 Signatures of weak (anti-)localization

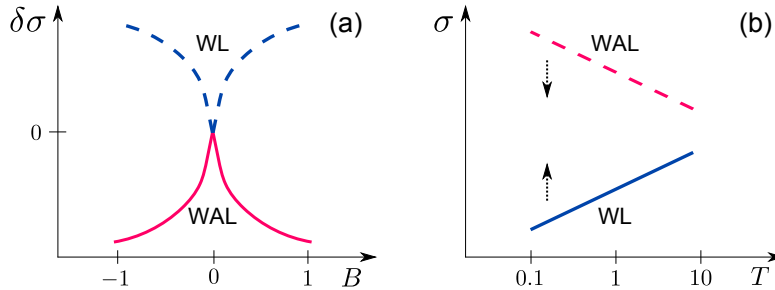


Figure 2. The signatures of weak localization (WL) and weak anti-localization (WAL) in two dimensions in (a) magnetoconductivity [defined as $\delta\sigma \equiv \sigma(B) - \sigma(0)$] and (b) temperature dependence of the conductivity σ . B is magnetic field and T is temperature. Adapted from Ref.³³

In two dimensions, the conductivity correction from the quantum interference takes the form of logarithmic function with ℓ_ϕ and ℓ serving as two cutoffs

$$\sigma^{qi} \propto \pm \frac{e^2}{\pi h} \ln \frac{\ell_\phi}{\ell} \quad (1)$$

where e^2/h is the conductance quantum, $-$ corresponds to weak localization and $+$ to weak anti-localization. Remind that ℓ is determined by the elastic scattering so it does not depend on temperature, while ℓ_ϕ is determined by the inelastic scattering so it is usually a function of temperature, and empirically,³⁴ $\ell_\phi \propto T^{-p/2}$, where p is positive and depends on dephasing mechanisms and dimensionality.²⁹

When lowering temperature, ℓ_ϕ could be longer and σ^{qi} will become prominent, this gives the temperature dependence of the conductivity as shown in Fig. 2 (b). Remember that σ^{qi} is from the quantum interference between time reversed scattering loops [see Fig. 1 (c)], so by applying a magnetic field that breaks time-reversal symmetry, σ^{qi} can be destroyed, giving rise to the magnetoconductivity [see Fig. 2 (a)].

2.3 Weak anti-localization in topological insulators

Since the studies of the carbon nanotube and graphene, it has been known that a two-dimensional gapless Dirac cone could have the weak anti-localization.^{13,14} The surface states of a three-dimensional topological insulator are also two-dimensional gapless Dirac fermions. The weak anti-localization was observed soon after the discovery of Bi_2Se_3 and Bi_2Te_3 as topological insulators (see Table 1). There is another reason that the weak anti-localization was observed easily. Because of poor sample quality, the mean free path is short in the materials, of the order of 10 nm. But the phase coherence length can reach up to 100nm to $1\mu\text{m}$ below the liquid helium temperature. In other words, these materials are in the quantum diffusion regime at low temperatures, where the weak (anti-)localization are supposed to occur.

In the experiments, the magnetoconductivity was fitted by the Hikami-Larkin-Nagaoka formula for conventional electrons,¹¹ with two fitting parameters: ℓ_ϕ the phase coherence length and α a prefactor of the order of

Table 1. The earlier experiments that observed the weak anti-localization in topological insulators. The magnetoconductivity measured was fitted by the Hikami-Larkin-Nagaoka formula¹¹ with two fitting parameters: the prefactor α and phase coherence length ℓ_ϕ . *Calculated from $B_\phi \equiv \hbar/(4e\ell_\phi^2)$. Adapted from Ref.³¹

Ref.	Sample	Thickness	T (K)	α	ℓ_ϕ (nm)
^{15,18}	Bi ₂ Se ₃	10~20 nm	0.3	-0.38	
¹⁶	Bi ₂ Se ₃	10 nm	1.8	-0.5~-0.38	106~237
¹⁷	Bi ₂ Se ₃	10 nm	1.8	-0.5~-0.38	106~237*
¹⁹	Bi ₂ Te ₃	50 nm	2	-0.39	331
²³	Bi ₂ Se ₃	2~6 QL	1.5	-0.39	75~200
²²	Bi ₂ Se ₃	45 nm	0.5	-0.31	1100
	(Bi,Pb)Se ₃			-0.35	640
²⁴	Bi ₂ Se ₃	5~20 nm	0.01~2	-1.1~-0.4	143~ ∞
²⁰	Bi ₂ Se ₃	3~100 QL	1.5	-0.63~-0.13	100~1000
²¹	Bi ₂ Se ₃	20 nm	0.3~100	-1.1~-0.7	15~300

1. α is positive for weak localization and negative for weak anti-localization. In the experiments, α covers a wide range between around -0.4 and -1.1, suggesting that the observed WAL can be interpreted by considering only one or two surface bands,^{15–24} despite of the coexistence of multiple carrier channels from bulk and surface bands at the Fermi surface. Even, the sharp WAL cusp can be completely suppressed by doping magnetic impurities only on the top surface of a topological insulator.¹⁹

3. WEAK ANTI-LOCALIZATION AND LOCALIZATION CROSSOVER

3.1 Theoretical formalism

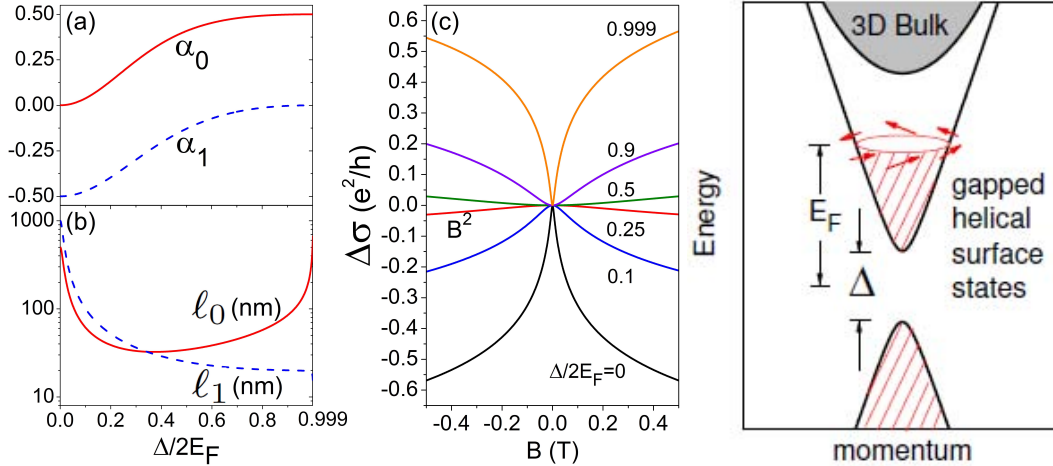


Figure 3. (a) WL (α_0) and WAL (α_1) weight factors as functions of $\Delta/2E_F$, where Δ is the gap, E_F is the Fermi energy. (b) WL (ℓ_0) and WAL (ℓ_1) lengths as functions of $\Delta/2E_F$. (c) Magnetoconductivity $\Delta\sigma(B)$ for different $\Delta/2E_F$ in the limit of weak magnetic scattering. (Right) The gapped surface states as massive Dirac fermions. $\ell_\phi = 300$ nm. Adapted from Ref.³⁰

The Dirac model in two dimensions is given by,^{4,35}

$$H = \gamma(\sigma \times \mathbf{k}) \cdot \hat{z} + \frac{\Delta}{2}\sigma_z, \quad (2)$$

where $\gamma = v\hbar$, v is the effective velocity, \hbar is the reduced Planck constant, $\sigma = (\sigma_x, \sigma_y)$ are the Pauli matrices, and $\mathbf{k} = (k_x, k_y)$ is the wave vector. H describes one conduction and one valence band, separated by a gap Δ [see Fig. 3 (right)]. We assume that the Fermi energy E_F crosses the conduction band. The spinor wave

function of the conduction band of H is given by $\psi_{\mathbf{k}}(\mathbf{r}) = (\cos \theta/2, -i \sin \theta/2 e^{i\varphi})^T e^{i\mathbf{k} \cdot \mathbf{r}}$, with $\cos \theta \equiv \Delta/2E_F$ and $\tan \varphi = k_y/k_x$.

The model can be applied to several different cases. (1) The gapless surface electrons with $\Delta = 0$.³⁶ (2) The massive surface states for a magnetically doped topological insulator with $\Delta \neq 0$.^{37,38} (3) The surface electrons in topological insulator thin films, where a finite gap is opened due to the finite size effect.³⁹ (4) The bulk electrons in topological insulator thin films where the mass term is the band gap between the conduction and valence band.³¹

The Berry phase is a geometric phase collected in an adiabatic cyclic process.^{40,41} The time-reversed scattering loops in Fig. 1 (c) are equivalent to moving an electron on the Fermi surface by one cycle. As a result, the electron picks up a Berry phase³⁰

$$\phi_b \equiv -i \int_0^{2\pi} d\varphi \left\langle \psi_{\mathbf{k}}(\mathbf{r}) \left| \frac{\partial}{\partial \varphi} \right| \psi_{\mathbf{k}}(\mathbf{r}) \right\rangle = \pi \left(1 - \frac{\Delta}{2E_F} \right). \quad (3)$$

The Berry phase can give an explanation to the weak anti-localization of two-dimensional Dirac fermions. In the massless limit, the Berry phase $\phi_b = \pi$, leading to a destructive quantum interference that suppresses the back scattering and enhances the conductivity, leading to the weak anti-localization.^{13,14} While in the large-mass limit, $\phi_b = 0$, which changes the quantum interference from destructive to constructive, resulting in the crossover to the weak localization,^{30,42,43} as shown in Fig. 3, as the Berry phase changes from π to 2π or 0.

The WAL-WL crossover can be depicted by the Lu-Shi-Shen formula for the magnetoconductivity³⁰

$$\Delta\sigma(B) = \sum_{i=0,1} \frac{\alpha_i e^2}{\pi h} \left[\Psi\left(\frac{\ell_B^2}{\ell_{\phi i}^2} + \frac{1}{2}\right) - \ln\left(\frac{\ell_B^2}{\ell_{\phi i}^2}\right) \right], \quad (4)$$

where Ψ is the digamma function, $\ell_B^2 \equiv \hbar/(4e|B|)$ is the magnetic length, $1/\ell_{\phi i}^2 \equiv 1/\ell_{\phi}^2 + 1/\ell_i^2$, ℓ_{ϕ} is the phase coherence length. The formula has two terms, one is for weak localization and the other is for weak anti-localization, characterized by two weight factors $\alpha_0 \in [0, 1/2)$ and $\alpha_1 \in [-1/2, 0)$, respectively. Sometimes α_i and ℓ_i were used by experiments as fitting parameters, but they are functions of $\Delta/2E_F$ [see Figs. 3(a) and (b)], so the Lu-Shi-Shen formula has only two fitting parameters $\Delta/2E_F$ and ℓ_{ϕ} .

3.2 Experimental verification

The crossover from weak anti-localization to weak localization was soon observed by many experiments, where the gap is opened mainly by two approaches: (1) Magnetically doped surface states. The surface states of topological insulator Bi_2Se_3 and Bi_2Te_3 are gapless because of time-reversal symmetry. By doping magnetic impurities that breaks time-reversal symmetry can open the gap, as has been observed by ARPES.^{37,38} The WAL-WL crossover has been observed in magnetically doped topological insulators, such as 3-quintuple-layer Cr-doped Bi_2Se_3 ,⁴⁴ Mn-doped Bi_2Se_3 ,⁴⁵ and $\text{EuS}/\text{Bi}_2\text{Se}_3$ bilayers.⁴⁶ After lowering the temperature below the Curie temperature, a crossover from WAL to WL is observed, indicating the relation between the ferromagnetism-induced gap opening and the crossover. (2) The finite-size effect of the surface states. In an ultrathin film of topological insulator, two gapless Dirac cones at the top and bottom surfaces can hybridize to open a finite-size gap, transforming the gapless Dirac cones into two massive Dirac cones.³⁹ For a given ultrathin film, the finite-size gap is fixed. But remember that the crossover depends on Δ/E_F , where E_F can be tuned by the gate voltage. Therefore, a WAL-WL crossover as a function of the gate voltage is observed in a 4-quintuple-layer $\text{Bi}_{1.14}\text{Sb}_{0.86}\text{Te}_3$.⁴⁷

4. WEAK LOCALIZATION OF BULK STATES

In most samples of topological insulator, the Fermi energy usually crosses not only the surface states, but also the bulk states [see Fig. 4(a)]. The localization behavior of the bulk states was a controversial topic.

The minimal model to describe a 3D topological insulator is the modified Dirac model³⁵

$$H_{3D} = \epsilon_{\mathbf{k}} + A\mathbf{k} \cdot \boldsymbol{\alpha} + \mathcal{M}_{\mathbf{k}}\beta, \quad (5)$$

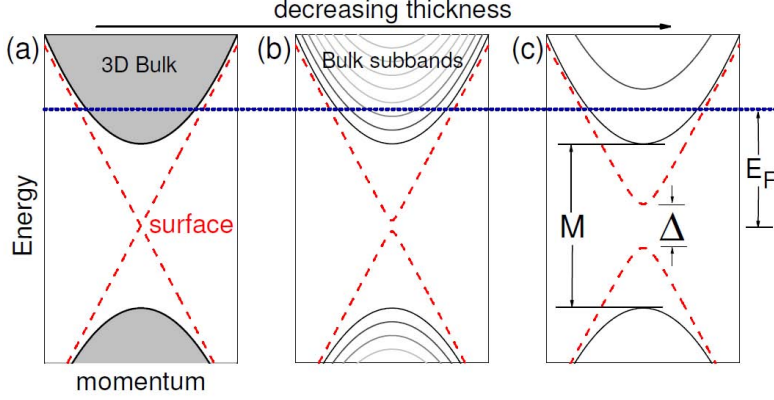


Figure 4. (a) The gapped bulk (grey area) and gapless surface (dashed lines) bands of a 3D topological insulator. (b) The quantum confinement along the z direction splits the 3D bulk bands into 2D subbands, while the hybridization of the top and bottom surfaces opens a gap (Δ) for the gapless surface bands. (c) In the ultrathin limit, the Fermi surface intersects with only one pair of bulk subbands (with band gap M) and one pair of gapped surface bands (each curve is two-fold degenerate). The horizontal dot line marks the Fermi energy E_F measured from the Dirac point. Adapted from Ref.³¹

where $\mathbf{k} = (k_x, k_y, k_z)$ are wavevectors, the 4×4 Dirac matrices can be expressed by the Pauli matrices $(\alpha_x, \alpha_y, \alpha_z) = \sigma_x \otimes (\sigma_x, \sigma_y, \sigma_z)$ and $\beta = \sigma_z \otimes \sigma_0$. $\epsilon_{\mathbf{k}} = C + D(k_z^2 + k^2)$, $\mathcal{M}_{\mathbf{k}} = m - B(k_z^2 + k^2)$, $k_{\pm} = k_x \pm ik_y$, and $k^2 = k_x^2 + k_y^2$. A, B, C, D , and m are model parameters. In a thin film of topological insulator, the 3D band structure split into 2D subbands. The simplest way to consider the lowest 2D bulk subbands in Figs. 4 (b) and (c) is to replace $\langle k_z \rangle = 0$ and $\langle k_z^2 \rangle = (\pi/d)^2$, where d is the thickness of the film. After defining $C + D(\pi/d)^2 = 0$, $M/2 \equiv m - B(\pi/d)^2$, the Hamiltonian of the lowest 2D bulk subbands can be written as

$$H = Dk^2 + \tau_z \left(\frac{M}{2} - Bk^2 \right) \sigma_z + A(\sigma_x k_x + \sigma_y k_y). \quad (6)$$

with $\tau_z = \pm 1$ is the block index. This is nothing but a modified two-dimensional Dirac model, up to a unitary rotation in $x - y$ plane compared to Eq. (2). At the band edge, the mass M is large compared to the Fermi energy [Fig. 4 (c)]. As a result, we expect that weak localization happens for the bulk states³¹ according to the Berry phase argument in the previous section. This result is quite different from other systems with strong spin-orbit interaction, where weak anti-localization is usually expected. This result was soon supported by other theoretical effort.⁴⁸ The crossover from weak anti-localization to localization can be realized by tuning the Fermi level or gate voltage in topological insulators. When the Fermi level is shifted from the bulk gap to the valence or conduction bands, there exist a competition between the bulk electrons and surface electrons. In this case, it is possible to observe the weak localization.

5. COMPARISON WITH CONVENTIONAL ELECTRONS

Table 2. Two-dimensional quantum diffusive transport of conventional and Dirac fermions in the presence of impurities of orthogonal (elastic), unitary (magnetic), and symplectic (spin-orbit) symmetries.⁴⁹ Adapted from Ref.³²

	Scalar scattering	Magnetic scattering	Spin-orbit scattering
Conventional electron	WL	both suppressed	WL \rightarrow WAL
Massless Dirac fermion	WAL	suppressed WAL	WAL
Dirac fermion in large-mass limit	WL	suppressed WL	suppressed WL

Either the weak localization or weak anti-localization has been observed in conventional two dimensional electron systems.²⁸ In conventional systems with dispersion of $p^2/2m$ and two-fold spin degeneracy on the Fermi surface, with only scalar disorder scattering, there will be weak localization. But strong spin-orbit scattering can leads to a crossover to the weak anti-localization,¹¹ because the spin-orbit scattering can bring the symplectic symmetry. For 2D gapless Dirac fermions, the symplectic symmetry is given by the band structure, so even with

only scalar disorder scattering, one can still expect weak anti-localization. By putting extra spin-orbit scattering will not change the symmetry, so there is still weak anti-localization. The difference is in the large-mass limit of the massive Dirac fermions, where the weak localization is sensitive to the spin-orbit scattering and will be suppressed.

Table 3. “Cooperon” channels for the conventional electrons and Dirac fermions. Triplet (singlet) channel gives WL (WAL). Spin-orbit scattering only quenches the triplet channels, leading to the crossover from WL to WAL for conventional electrons and the suppression of WL in the large-mass limit of Dirac fermions. Adapted from Ref.³²

Cooperon channels	“Triplet”(⇒WL)	“Singlet”(⇒WAL)
Conventional electron	×3	×1
Massless Dirac fermion	×0	×1
Large-mass Dirac fermion	×1	×0

A deeper understanding can be found in Table 3. The theory of weak localization can be equivalent to the diffusive transport of the Cooperon, a quasiparticle formed by pairing the electronic states before and after the back scattering. For conventional electrons, the pairing of two spin 1/2 electrons can form 3 triplet Cooperon channels with total angular momenta $j = 1$ and one singlet Cooperon channel with $j = 0$.⁵⁰ Each channel of the triplets gives the weak localization, while the singlet channel gives the weak anti-localization. Because the triplets outnumber the singlet, we usually have the weak localization. However, the spin-orbit scattering behaves like a spin-dependent magnetic scattering, it can destroy the triplet Cooperon channels because they have a nonzero angular momentum, while has no effect on the singlet Cooperon channel. As a result, in the presence of strong spin-orbit scattering, one expects a crossover from weak localization to weak anti-localization.

Different from the conventional electrons, the massive Dirac model is a superposition of one singlet and one “triplet”,³² in the massless and large-mass limits, respectively (see Table 3). As a result, the weak localization in the large-mass limit can be destroyed by the spin-orbit scattering.

6. INTERACTION-INDUCED LOCALIZATION OF SURFACE ELECTRONS

6.1 Transport paradox in measurements

One of the merits of topological insulators was thought to be that their topologically protected surface states could not be localized.^{1,2} This is based on a property of two-dimensional massless and non-interacting Dirac fermions in the thermodynamic limit.^{7,8} For a long time the cusp of negative magnetoconductivity serves as an precursor of this delocalization tendency.

However, although a negative magnetoconductivity as the signature of the weak anti-localization has been observed in most topological insulator samples, the temperature dependence of the conductivity does not indicate its corresponding enhanced conductivity with decreasing temperature (see Fig. 2) as expected for weak anti-localization. Instead, in most experiments, a suppression of the conductivity with decreasing temperature is observed,^{22–27} indicating a behavior of the weak localization, which is supposed to happen in ordinary disordered metals as a precursor of the Anderson localization.^{28,29} In these samples, the bulk states coexist with the surface states, so the bulk states may contribute to the localization. However, if the surface states could not be localized, the total conductivity should saturate at a critical temperature, but this is not the experimental measurement. Thus experimental observation in magnetoconductance and finite temperature conductance presents a transport paradox in topological insulators.

6.2 Theory of interaction effect

The transport paradox cannot be reconciled in the theory of the quantum interference correction (σ^{qi}) to the conductivity. The electron-electron interaction^{51,52} (σ^{ee}) provides a possible way to understand the unexpected temperature dependence.³³ Figure 5 compares σ^{ee} and σ^{qi} as functions of temperature at different magnetic fields, for the parameters comparable with those in the experiments. With or without the magnetic field, σ^{ee} decreases logarithmically with decreasing temperature [Figure 5 (a)], showing a localization tendency, much like in usual two-dimensional disordered metals.^{51,52} In contrast, zero-field σ^{qi} enhances the conductivity when

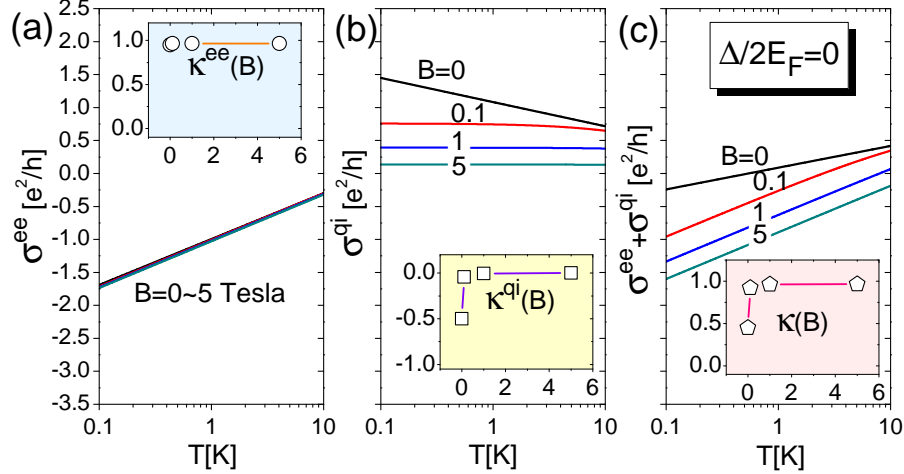


Figure 5. The conductivity corrections from the electron-electron interaction (σ^{ee}) and quantum interference (σ^{qi}) as functions of temperature T at different perpendicular magnetic fields B . Insets show the slopes $\kappa(B) \equiv (\pi h/e^2) \partial \sigma / \partial \ln T$ at $T = 1$ K as functions of B . The parameters are adopted from those in the topological insulators Bi_2Se_3 and Bi_2Te_3 : $\Delta/2E_F = 0$, $\gamma = 3$ eVÅ, the relative permittivity⁵³ $\epsilon_r = 100$, the mean free path $\ell = 10$ nm, and the phase coherence length is taken to be $\ell_\phi = 700 T^{-p/2}$ nm with T in units of Kelvin and $p = 1$.^{16,18} Adapted from Ref.³³

lowering temperature and is suppressed by the magnetic field [Figure 5 (b)], a typical behavior of the weak anti-localization. The contribution from σ^{ee} is stronger, so the overall temperature dependence of the conductivity shows a weak localization tendency [Figure 5 (c)], consistent with the experimental observations.

Table 4. The slope $\kappa \equiv (\pi h/e^2) \partial \sigma / \partial \ln T$ in experiments. σ is the conductivity. The change of slope $\delta\kappa \equiv \kappa(B_c) - \kappa(0)$. Above a critical magnetic field, the slope saturates. n is the sheet carrier density. n for C and D are converted from their cubic carrier densities.

Experiment	A ²⁴	B ₁ ²²	B ₂ ²²	C ²⁵	D ²⁶	E ²⁷
Compound	Bi_2Se_3	Bi_2Se_3	$\text{Pb}_x\text{Bi}_{2-x}\text{Se}_3$	$\text{Cu}_x\text{Bi}_{2-x}\text{Se}_3$	Bi_2Te_3	Bi_2Te_3
n [$10^{12}/\text{cm}^2$]	$20e^-$	$102e^-$	$49.5e^-$	$6.72e^-$	$37h^+$	$120e^-$
Thickness [nm]	10	45	45	80	65	4
$\kappa(B=0)$	0.68	0.86	0.70	1.37	1.33	0.58
$\kappa(B=0.2)$	0.8	-	-	-	-	0.89
$\kappa(B=0.5)$	-	-	-	-	-	0.98
$\kappa(B=1)$	0.8	-	-	-	-	1.04
$\kappa(B=2)$	0.8	1.18	1.29	1.68	-	1.07
$\kappa(B=3)$	0.8	-	-	1.66	-	-
$\kappa(B=5)$	0.8	-	-	1.67	1.66	1.09
$\delta\kappa$	0.12	0.32	0.58	0.30	0.33	0.51

The temperature dependence of the conductivity is characterized by the slope

$$\kappa \equiv \frac{\pi h}{e^2} \frac{\partial \sigma}{\partial \ln T}. \quad (7)$$

We summarize the data of κ in several recent experiments (Tab. 4), where κ is always positive; and by applying a magnetic field, κ increases then saturates after B exceeds a saturation field B_ϕ . Compared with the experiments, the results presented in Fig. 5 agree well with the experiments, with comparable change of the conductivity (several e^2/h), temperatures (0.1 to 10 K) and magnetic fields (0 to 5 Tesla).²²⁻²⁷

In this way, we show that the two-dimensional massless Dirac fermions will intend to be localized when the electron-electron interaction and disorder scattering are taken into account.

7. SUMMARY

In summary, we developed a quantum transport theory for two-dimensional massive Dirac fermions by considering the disorder scattering up to the quantum interference correction and the interplay with electron-electron interaction. The theory has been successfully applied to account for transport measurements in the topological insulators, it (1) predicted the crossover between weak anti-localization and weak localization as the surface states of topological insulators acquires a mass in the case of magnetic doping or in the case of thin film; (2) shows that the bulk states in a topological insulator thin film could have weak localization, in contrast to other systems with strong spin-orbit interaction; (3) clarifies the Cooperon channels for the 2D massive Dirac fermions and their responses to disorders of different symmetries; (4) reconciles the experimentally observed transport paradox in topological insulators: coexistence of weak localization tendency in the temperature dependence of the conductivity and the weak anti-localization behavior in the magnetoconductivity.

The decreasing conductivity in $\ln T$ at low temperatures indicates the weak localization of the surface electrons in topological insulators. Theoretically the surface electrons “inherits” topological properties from the bulk band structures. The bulk-surface correspondence manifests the existence of the surface electrons surrounding the boundary of a topological insulator. It was extensively accepted¹⁻³ that when disorders and impurities are added at the surface, there will be scattering between these surface electrons, but they cannot become localized. The electron-electron interaction makes it different: the surface electrons can be localized at low temperatures in an interacting topological insulator. The topological classification of topological insulators and superconductors is based on the framework of random matrix theory, which is essentially a single-particle problem.⁵⁴ The theory is based on the symmetries in a single particle Hamiltonian, and predicts the existence of at most five classes of topological insulators and superconductors in each dimension. Thus the classification is limited to the non-interacting systems. Introduction of disorders and impurities still keeps the square matrix property of the Hamiltonian, and does not destroy the validity of topological classification if the disorders and impurity does not break the symmetry. However, the electron-electron interaction leads to a many-body problem. Thus the weak localization of surface electrons in a topological insulator brings us an important issue on the robustness of a topological phase in an interacting system, which deserves to be investigated furthermore.

ACKNOWLEDGMENTS

This work was supported by Research Grant Council of Hong Kong under Grant No.: HKU 7051/11P.

REFERENCES

1. Moore, J. E., “The birth of topological insulators”, *Nature* **464**, 194-198 (2010).
2. Hasan, M. Z. and Kane, C. K., “Topological insulators”, *Rev. Mod. Phys.* **82**, 3045-3067 (2010).
3. Qi, X. L. and Zhang S. C., “Topological insulators and superconductors”, *Rev. Mod. Phys.* **83**, 1057-1110 (2011).
4. Shen, S. Q., “Topological insulators” (Springer, Berlin, 2012).
5. Xia, Y., Qian, D., Hsieh, D., Wray, L., Pal, A., Lin, H., Bansil, A., Grauer, D., Hor, Y. S., Cava, R. J. and Hasan, M. Z., “Observation of a large-gap topological-insulator class with a single Dirac cone on the surface”, *Nat. Phys.* **5**, 398 (2009).
6. Ando, T., Nakanishi, T., and Saito, R., “Berry’s phase and absence of backscattering in carbon nanotubes”, *J. Phys. Soc. Jpn.* **67**, 2857 (1998).
7. Bardarson, J. H., Tworzydło, J., Brouwer, P. W. and Beenakker, C. W. J., “One-parameter scaling at the Dirac point in graphene”, *Phys. Rev. Lett.* **99**, 106801 (2007).
8. Nomura, K., Koshino, M. and Ryu, S., “Topological delocalization of two-dimensional massless Dirac fermions”, *Phys. Rev. Lett.* **99**, 146806 (2007).
9. Culcer, D., “Transport in three-dimensional topological insulators: Theory and experiment”, *Physica E* **44**, 860-884 (2012).
10. Bardarson, J. H. and Moore, J. E., “Quantum interference and Aharonov-Bohm oscillations in topological insulators”, *Rep. Prog. Phys.* **76**, 056501 (2013).

11. Hikami, S., Larkin, A. and Nagaoka, Y., "Spin-orbit interaction and magnetoresistance in the two dimensional random system", *Prog. Theor. Phys.* **63**, 707 (1980).
12. Shen, S. Q., "Spin Hall effect and Berry phase in two dimensional electron gas", *Phys. Rev. B* **70**, 081311 (R) (2004).
13. Suzuura, H. and Ando, T., "Crossover from symplectic to orthogonal class in a two-dimensional honeycomb lattice", *Phys. Rev. Lett.* **89**, 266603 (2002).
14. McCann, E., Kchedzhi, K., Fal'ko, V. I., Suzuura, H., Ando, T. and Altshuler, B. L., "Weak-localization magnetoresistance and valley symmetry in graphene", *Phys. Rev. Lett.* **97**, 146805 (2006).
15. Checkelsky, J. G., Hor, Y. S., Liu, M. H., Qu, D. X., Cava, R. J. and Ong, N. P., "Quantum interference in macroscopic crystals of nonmetallic Bi_2Se_3 ", *Phys. Rev. Lett.* **103**, 246601 (2009).
16. Peng, H. L., Lai, K. J., Kong, D. S., Meister, S., Chen, Y. L., Qi, X. L., Zhang, S. C., Shen, Z. X. and Cui, Y., "Aharonov-Bohm interference in topological insulator nanoribbons", *Nature Mater.* **9**, 225-229 (2010).
17. Chen, J., Qin, H. J., Yang, F., Liu, J., Guan, T., Qu, F. M., Zhang, G. H., Shi, J. R., Xie, X. C., Yang, C. L., Wu, K. H., Li, Y. Q. and Lu, L., "Gate-voltage control of chemical potential and weak antilocalization in Bi_2Se_3 ", *Phys. Rev. Lett.* **105**, 176602 (2010).
18. Checkelsky, J. G., Hor, Y. S., Cava, R. J. and Ong, N. P., "Bulk band gap and surface state conduction observed in voltage-tuned crystals of the topological insulator Bi_2Se_3 ", *Phys. Rev. Lett.* **106**, 196801 (2011).
19. He, H. T., Wang, G., Zhang, T., Sou, I. K., Wong, G. K. L., Wang, J. N., Lu, H. Z., Shen, S. Q. and Zhang, F. C., "Impurity effect on weak antilocalization in the topological insulator Bi_2Te_3 ", *Phys. Rev. Lett.* **106**, 166805 (2011).
20. Kim, Y. S., Brahlek, M., Bansal, N., Edrey, E., Kapilevich, G. A., Iida, K., Tanimura, M., Horibe, Y., Cheong, S. W., and Oh, S., "Thickness-dependent bulk properties and weak antilocalization effect in topological insulator Bi_2Se_3 ", *Phys. Rev. B* **84**, 073109 (2011).
21. Steinberg, H., Laloe, J. B., Fatemi, V., Moodera, J. S., and Jarillo-Herrero, P., "Electrically tunable surface-to-bulk coherent coupling in topological insulator thin films", *Phys. Rev. B* **84**, 233101 (2011).
22. Wang, J., DaSilva, A. M., Chang, C. Z., He, K., Jain, J. K., Samarth, N., Ma, X. C., Xue, Q. K. and Chan, M. H. W., "Evidence for electron-electron interaction in topological insulator thin films", *Phys. Rev. B* **83**, 245438 (2011).
23. Liu, M., Chang, C. Z., Zhang, Z., Zhang, Y., Ruan, W., He, K., Wang L. L., Chen, X., Jia, J. F., Zhang, S. C., Xue, Q. K., Ma, X. C. and Wang, Y., "Electron interaction-driven insulating ground state in Bi_2Se_3 topological insulators in the two-dimensional limit", *Phys. Rev. B* **83**, 165440 (2011).
24. Chen, J., He, X. Y., Wu, K. H., Ji, Z. Q., Lu, L., Shi, J. R., Smet, J. H. and Li, Y. Q., "Tunable surface conductivity in Bi_2Se_3 revealed in diffusive electron transport", *Phys. Rev. B* **83**, 241304(R) (2011).
25. Takagaki, Y., Jenichen, B., Jahn, U., Ramsteiner, M. and Friedland, K. J., "Weak antilocalization and electron-electron interaction effects in Cu-doped Bi_2Se_3 films", *Phys. Rev. B* **85**, 115314 (2012).
26. Chiu, S. P. and Lin, J. J., "Weak antilocalization in topological insulator Bi_2Te_3 microflakes", *Phys. Rev. B* **87**, 035122 (2013).
27. Roy, A., Guchhait, S., Sonde, S., Dey, R., Pramanik, T., Rai, A., Movva, H. C. P., Colombo, L. and Banerjee, S. K., "Two-dimensional weak anti-localization in Bi_2Te_3 thin film grown on $\text{Si}(111)-(7\times 7)$ surface by molecular beam epitaxy", *Appl. Phys. Lett.* **102**, 163118 (2013).
28. Bergmann, G., "Weak localization in thin films: a time-of-flight experiment with conduction electrons", *Phys. Rep.* **107**, 1 (1984).
29. Lee, P. A. and Ramakrishnan, T. V., "Disordered electronic systems", *Rev. Mod. Phys.* **57**, 287-337 (1985).
30. Lu, H. Z., Shi, J. and Shen, S. Q., "Competition between weak localization and antilocalization in topological surface states", *Phys. Rev. Lett.* **107**, 076801 (2011).
31. Lu, H. Z. and Shen, S. Q., "Weak localization of bulk channels in topological insulator thin film", *Phys. Rev. B* **84**, 125138 (2011).
32. Shan W. Y., Lu, H. Z. and Shen, S. Q., "Spin-orbit scattering in quantum diffusion of massive Dirac fermions", *Phys. Rev. B* **86**, 125303 (2012).
33. Lu, H. Z. and Shen S. Q., "Finite-temperature conductivity and magnetoconductivity of topological insulators", *Phys. Rev. Lett.* **112**, 146601 (2014).

34. Thouless, D. J., "Maximum metallic resistance in thin wires", Phys. Rev. Lett. **39**, 1167-1169 (1977).
35. Shen, S. Q., Shan, W. Y. and Lu, H. Z., "Topological insulator and the Dirac equation", SPIN **1**, 33 (2011).
36. Shan, W. Y., Lu, H. Z., and Shen, S. Q., "Effective continuous model for surface states and thin films of three-dimensional topological insulator", New J. Phys. **12**, 043048 (2010).
37. Chen, Y. L., Chu, J. H., Analytis, J. G., Liu, Z. K., Igarashi, K., Kuo, H. H., Qi, X. L., Mo, S. K., Moore, R. G., Lu, D. H., Hashimoto, M., Sasagawa, T., Zhang, S. C., Fisher, I. R., Hussain, Z., Shen, Z. X., "Massive Dirac fermion on the surface of a magnetically doped topological insulator", Science **329**, 659 (2010).
38. Wray, L. A., Xu, S. Y., Xia, Y. Q., Hsieh, D., Fedorov, A. V., Hor, Y. S., Cava, R. J., Bansil, A., Lin, H., and Hasan, M. Z., "A topological insulator surface under strong Coulomb, magnetic and disorder perturbations", Nature Phys. **7**, 32 (2011).
39. Lu, H. Z., Shan, W. Y., Yao, W., Niu, Q., and Shen, S. Q., "Massive Dirac fermions and spin physics in an ultrathin film of topological insulator", Phys. Rev. B **81**, 115407 (2010).
40. Pancharatnam, S., "Generalized theory of interference, and its applications. Part I. Coherent pencils", Proc. Indian Acad. Sci. A **44**, 247-262 (1956).
41. Berry, M. V., "Quantal phase factors accompanying adiabatic changes", Proceedings of the Royal Society A **392**, 45-57 (1984).
42. Ghaemi, P., Mong, R. S. K. and Moore, J. E., "In-plane transport and enhanced thermoelectric performance in thin films of the topological insulators Bi₂Te₃ and Bi₂Se₃", Phys. Rev. Lett. **105**, 166603 (2010).
43. Imura, K., Kuramoto, Y. and Nomura, K., "Weak localization properties of the doped Z₂ topological insulator", Phys. Rev. B **80**, 085119 (2009).
44. Liu, M., Zhang, J., Chang, C. Z., Zhang, Z., Feng, X., Li, K., He, K., Wang, L. L., Chen, X., Dai, X., Fang, Z., Xue, Q. K., Ma, X. and Wang, Y., "Crossover between weak antilocalization and weak localization in a magnetically doped topological insulator", Phys. Rev. Lett. **108**, 036805 (2012).
45. Zhang, D., Richardella, A., Rench, D. W., Xu, S. Y., Kandala, A., Flanagan, T. C., Beidenkopf, H., Yeats, A. L., Buckley, B. B., Klimov, P. V., Awschalom, D. D., Yazdani, A., Schiffer, P., Hasan, M. Z. and Samarth, N., "Interplay between ferromagnetism, surface states, and quantum corrections in a magnetically doped topological insulator", Phys. Rev. B **86**, 205127 (2012).
46. Yang, Q. I., Dolev, M., Zhang, L., Zhao, J., Fried, A. D., Schemm, E., Liu, M., Palevski, A., Marshall, A. F., Risbud, S. H. and Kapitulnik, A., "Emerging weak localization effects on topological insulator-insulating ferromagnet (Bi₂Se₃-EuS) interface", Phys. Rev. B **88**, 081407(R) (2013).
47. Lang, M., He, L., Kou, X., Upadhyaya, P., Fan, Y., Chu, H., Jiang, Y., Bardarson, J. H., Jiang, W., Choi, E. S., Wang, Y., Yeh, N. C., Moore, J. and Wang, K. L., "Competing weak localization and weak antilocalization in ultrathin topological insulators", Nano Lett. **13**, 48 (2013).
48. Garate, I. and Glazman, L., "Weak localization and antilocalization in topological insulator thin films with coherent bulk-surface coupling", Phys. Rev. B **86**, 035422 (2012).
49. Dyson, F. J., "Statistical theory of the energy levels of complex systems. I", J. Math. Phys. (N.Y.) **3**, 140 (1962).
50. Altshuler, B. L., Aronov, A. G., Larkin, A. I., and Klmel'nitskii, D. E., "Anomalous magnetoresistance in semiconductors", JETP **54**, 411 (1981).
51. Altshuler, B. L., Aronov, A. G., and Lee, P. A., "Interaction effects in disordered Fermi systems in two dimensions", Phys. Rev. Lett. **44**, 1288-1291 (1980).
52. Fukuyama, H., "Effects of interactions on non-metallic behaviors in two-dimensional disordered systems", J. Phys. Soc. Jpn. **48**, 2169-2170 (1980).
53. Richter, W., Kohler, H., and Becker, C. R., "A Raman and far-infrared investigation of phonons in the rhombohedral V₂-VI₃ compounds Bi₂Te₃, Bi₂Se₃, Sb₂Te₃ and Bi₂(Te_{1-x}Se_x)₃ (0 < x < 1), (Bi_{1-y}Sb_y)₂Te₃ (0 < y < 1)", Phys. Status Solidi (b) **84**, 619 (1977).
54. Schnyder, A. P., Ryu, S., Furusaki, A., and Ludwig, A. W. W., "Classification of topological insulators and superconductors in three spatial dimensions", Phys. Rev. B **78**, 195125 (2008).